

Measuring Entropy in Mesoscopic Circuits

by

Owen Sheekey

A THESIS SUBMITTED IN PARTIAL FULFILLMENT
OF THE REQUIREMENTS FOR THE DEGREE OF

Honours Bachelors of Science

in

THE FACULTY OF SCIENCE

(Physics)

The University of British Columbia

(Vancouver)

April 2021

© Owen Sheekey, 2021

Abstract

We have tested whether the entropy of a quantum system can be measured non-locally, using a capacitively coupled quantum dot as a sensor. We have extended upon the research already done in mesoscopic circuits showing that the entropy of the first few electron ground states in a quantum dot can be locally measured directly. To demonstrate whether this local measurement can be extended to measure the entropy of a nonlocal quantum system, we have probe a simple two state system made up of an electron in a superposition between a quantum dot and a reservoir. Entropy measurements were completed by capacitively coupling this two-state system to a probe quantum dot whose occupation affects the degeneracy of the two-state system and by extension, its entropy. In the dot acting as the probe dot, change in entropy of the entire system was measured by measuring shifts in the occupancy transition from 0 to 1 electrons as a function of temperature. By showing that we can measure the entropy of a quantum system nonlocally — or by measuring only the properties of a nearby, coupled quantum dot — we provide a path to distinguish more novel entangled states with unique entropies.

Table of Contents

Abstract	ii
Table of Contents	iii
List of Tables	v
List of Figures	vi
Glossary	x
Acknowledgments	xi
1 Introduction	1
2 Entropy in mesoscopic systems	3
2.1 Entropy of small quantum systems	3
2.2 From a Maxwell relation to entropy in a single quantum dot	3
2.3 Free energy explanation	6
3 Capacitively coupled double quantum dot	7
3.1 Quantum dots in GaAs/AlGaAs heterostructures	7
3.2 The device and measurement protocol	7
3.3 Results	9
3.4 Comparison to theory	10
3.5 Conclusion	10

Bibliography	16
A Measurement technique	18
A.1 Heating	18
A.2 Extraction of dN/dT signal	18
A.3 Artifacts from cross couplings	18
A.4 Determination of electron temperature	19
B Measurement setup	20
C Device Fabrication	21

List of Tables

List of Figures

Figure 2.1	In (a) and (b) we show two examples of the measurement protocol where the occupancy of the probe dot is measured using G_{sens} . In each case, the occupancy is swept from $N - 1$ to N electrons both at a higher temperature (red) and a lower temperature (blue), however in (a) this change in N does not correspond to an entropy change in the system whereas in (b) we see a positive change in entropy of the system due to this change in occupancy. The inlaid plots show the cumulative integral of dG_{sens} – or the difference between hot and cold G_{sens} curves. The entropy change of the system is measured by the value of this integral after the completion of this transition. V_{mid} is labelled for each curve, notably, V_{mid} is the same in the zero entropy case, but shifts in the finite entropy case. Figure from Hartman et al.	6
------------	--	---

Figure 3.1	The states of the double quantum dot system are mapped out by charge sensing the occupation of both dots. The color indicates the derivative of the current through the charge sensor. Sudden changes in this current indicate state changes in the two dots, with larger changes (seen as darker on this plot) indicating changes in the probe dot, and smaller changes (slightly lighter on this plot) indicating changes in states in the impurity dot. The large squares indicate regions of constant state in the two dots and are labelled by [occupation main dot, occupation impurity dot].	8
Figure 3.2	A top-down SEM image of the device measured in this experiment. Lighter gold regions are the gold gates, while darker regions are the GaAs substrate. A single quantum dot (right hand side) is probed by the leftmost dot whose occupation is measured using I_{sens} . In this device, temperature oscillations occur across electrons in a reservoir connected to the probe dot heated via a small thermocurrent through an adjacent quantum point contact. V_{ACC} is used to control the chemical potential, μ , in the probe dot. In the right hand of dot, similar gate structures, labelled V_{IP} allow for the system to be tuned to be tuned degenerate with the probe dot. The X indicates ohmic contact to the 2DEG. The light red section indicates the thermal reservoir of the system. Greyed out gates were not used in this experiment.	11

Figure 3.3	Entropy along the $0,1 \rightarrow 1,0$ transition in the pair of dots with $\Gamma_{main}/T < 1 < \Gamma_{imp}/T$. In (a) the dark region indicates the transition in the main quantum dot. Double dot states are labelled as [Occupation main dot, occupation impurity dot]. The ΔS of the transition in the main dot is plotted for the double dot transition crossing. In the $0,0 \rightarrow 1,0$ regime, the ΔS is found to be roughly $\ln 2 \approx 0.69$ as expected from the spin degeneracy in the probe dot. In the central regime, where there is a full $0,1 \rightarrow 1,0$ transition, entropy is found to be around $\ln 2 - \ln 2 = 0$ since the spin degeneracy of the impurity dot is simply replaced by the spin degeneracy in the probe dot. In (b) the ΔI between the cold and hot curves plotted in (c) are shown. In (c) the shift in V_{mid} between 70 mK and 50 mK traces can clearly be seen to vary depending on ΔS	12
Figure 3.4	Data from an older device exhibits a change in entropy as degeneracy of an unknown external impurity is adjusted. The demonstrates the potential for measuring the entropy of capacitively coupled systems.	13
Figure 3.5	Theoretical calculations of ΔS across the $01 \rightarrow 10$ transition are show for various levels of interdot capacitive coupling to temperature ratios. Excellent alignment with experiment is achieved in the $U/T = 6$ are achieved.	14
Figure 3.6	A cross section of the GaAs/AlGaAs heterostructure hosting a 2-dimensional electron gas (2DEG) formed at the boundary between an AlGaAs and GaAs layer where the conductance band briefly falls below the Fermi energy [3]. Gold gates allow local control of the electron density of the 2DEG. Ohmic contact to the 2DEG is established by a diffusion of a combination of Ni/Au/Ge from the surface to the 2DEG.	15

Figure A.1 By fitting the transition line shapes of the $0 \rightarrow 1$ electron transition in the quantum dot, one can extract the broadening of the fermi energy in the reservoir. By varying the lattice temperature of the substrate and plotting the effective broadening of the fermi sea (θ) at each lattice temperature, we can extract the effective electron temperature, T_e . Here $T_e \approx 35$ mK. . . . 19

Glossary

This glossary uses the handy `acroynym` package to automatically maintain the glossary. It uses the package's `printonlyused` option to include only those acronyms explicitly referenced in the `LATEX` source.

Acknowledgments

I would first like to thank all the students in Josh Folk's lab for all they have done for this project and for all they have taught me about being an experimentalist. Christian Olsen, who was patient while I was first learning how to do anything useful in the lab. Manab Kuiri, who discussed physics with me everyday, and is always up to date on all the newest results. And of course, Tim Child, without whom this project would not have been possible.

More here.

Chapter 1

Introduction

In the past few decades, significant advances in the field of quantum transport have yielded a large number of interesting quantum systems and effects including Majorana bound states [7], the 2-channel Kondo effect [10], and the $\nu = 5/2$ fractional quantum hall state [16]. All of these systems have been well characterized using traditional transport techniques. However, if we were able to measure the entropy of mesoscopic quantum systems like these, we would be able to more clearly distinguish them from trivial states, and perhaps detect deviations from theory in ways which traditional transport measurements do not allow. Of particular interest is the Majorana bound state whose characteristics make it especially well suited to the field of quantum computing [1, 8], but whose transport signature is suspiciously close to that of the much less interesting (and less useful) Andreev bound state [15]. It has been proposed that the entropy of such a Majorana bound state would significantly differ from that of an Andreev bound state [14]. However, in the past, entropy measurements of systems like these were never possible because of limitations of techniques which rely on heat capacity and other macroscopic quantities which can be experimentally difficult to measure for localized quantum states.

A few years ago, Hartman et al. [5] showed that it is possible to measure the entropy of a single spin $\frac{1}{2}$ particle in a quantum dot, opening the possibility of introducing entropy as a new technique for characterization of more interesting mesoscopic quantum systems, like those mentioned above. To complete their measurement, Hartman et al. measured electronic occupation in a few-electron quantum dot at

varying temperatures, relating this quantity to entropy following a Maxwell relation. Recently, schemes similar to the one realized in this experiment have been used to measure entropy in magic angle (twisted bilayer) graphene [11, 12]. Both measurements have shown remarkable evidence of an effective “freezing” of electrons as temperature is increased – analogous to the Pomeranchuk effect in ^3He [9]. The results of these recent experiments further illustrate the value in measurements of entropy in quantum materials to provide insights into the electronic states of the system.

In this thesis, we present data to show that the measurement protocol using a single few-electron quantum dot introduced by Hartman et al. to measure the entropy of a single spin $\frac{1}{2}$ can be extended to measure the entropy of an additional capacitively coupled quantum system. We provide evidence that, when occupation of a single few-electron quantum dot affects the degeneracy of a larger thermodynamic system, the change in entropy of the entire system can be measured while only measuring the occupation of the single quantum dot.

Chapter 2

Entropy in mesoscopic systems

In this chapter, we review the theoretical underpinnings for the measurements that were completed. First, we discuss some of the theory behind single and double quantum dots and the relevant energy scales for these systems. We then proceed to a review of entropy in quantum systems, finally discussing the Maxwell relation used to make the measurements of entropy presented in this thesis and those presented by Hartman et al.

2.1 Entropy of small quantum systems

The classical description of entropy comes in the form of the Boltzmann entropy

$$S = k_b \ln W. \quad (2.1)$$

Here, W is defined by the number of available microstates of the system [13]. In the

2.2 From a Maxwell relation to entropy in a single quantum dot

To measure the entropy of a system using a mesoscopic circuit, we use the Maxwell relation and resulting integral.

$$\left(\frac{\partial \mu}{\partial T}\right)_{p,N} = -\left(\frac{\partial S}{\partial N}\right)_{p,T}, \quad \Delta S = \int_{\mu_1}^{\mu_2} \frac{dN(\mu)}{dT} d\mu \quad (2.2)$$

In other words, by measuring the occupation of a quantum dot as a function of the chemical potential, $N(\mu)$, and varying temperature, T , we can derive the change in entropy, ΔS over that change in occupation.

In systems with few degrees of freedom, the relevant discussion of entropy comes in the form of Boltzmann entropy, $S = k_b \ln \Omega$ with Ω being the number of available microstates [13]. In Hartman et al.'s experiment, it was shown that the change in entropy as a quantum dot goes from an occupation of $0 \rightarrow 1$ electrons was $\Delta S = k_b \ln 2 - k_b \ln 1 = k_b \ln 2$ as the dot went from only having one possible state to having two possible spin states (spin up and spin down). In addition, it was shown that by applying a large magnetic field, Zeeman splitting of the energy levels in the dot eliminated this degeneracy causing $\Delta S = k_b \ln 1 - k_b \ln 1 = 0$.

In practice, to measure the entropy of a small system using a mesoscopic circuit and the integral from Eqn. 2.2 we have a few requirements. First, we assumed constant pressure in the Maxwell relation. In the context of a 2-dimensional electron gas (2DEG) with which our measurements are conducted, the dominating pressure at temperatures below the Fermi temperature, $T_F \approx 100\text{K}$ is the degeneracy pressure [2], an incompressibility emerging from the Pauli exclusion principle disallowing fermions from occupying the same quantum state. In addition, by keeping energy fluctuations due to thermal energy, $k_b T$, much smaller than the spacing between energy levels in the dot, we ensure that random temperature fluctuations do not produce unpredictable energy level occupation. To carry out the integration from Eqn. ?? in practice, it is necessary to have an accurate way of measuring the occupancy, N , of the probe dot. We measure N by measuring the conductance G_{sens} through a charge sensing quantum point contact (QPC) seen in Fig. 3.2.

Because of the proximity of this QPC, referred to as the charge sensor, to the probe dot very small electrostatic changes in the probe dot affect the conduction across the charge sensor [4]. As such, a larger G_{sens} indicates fewer electrons in the probe dot, while a smaller G_{sens} indicates more electrons in the probe dot. In effect, this means that G_{sens} can be used to directly measure the occupancy of the dot as a function of various other quantities like chemical potential, μ , or temperature, T .

We use $V_{plunger}$ (V_p) shown in in Fig. 3.2 to locally control the chemical potential of the dot. Varying the potential applied to this gate V_p - and by extension the chemical potential in the dot - is our primary technique to control the occupancy of the dot. Based on this protocol, we can decompose Eqn. ?? into the following quantities which can be determined experimentally.

$$\Delta S = \int_{\mu_1}^{\mu_2} dG_{sens} \frac{dN}{dG_{sens}} \frac{1}{dT} d\mu \quad (2.3)$$

This integral tells us that we can measure the change in entropy between two chemical potentials in the dot by measuring three quantities: dN/dG_{sens} , dT , and dG_{sens} as a function of chemical potential. The first two quantities dN/dG_{sens} and dT are scaling factors that can be independently experimentally determined but do not depend on μ however the final quantity dG_{sens} does depend on μ and so must be measured as μ is changed. Intuitively, dG_{sens} is a measure of the difference between the occupancy of the dot at higher T and lower T - this is illustrated by the shading on the plots in Fig. 2.1.

Using $V_{degeneracy}$ (V_d) the quantum system composed of the two dots (highlighted in yellow in Fig. 3.2) with a single electron confined within the system can be tuned between non-degenerate and doubly-degenerate. This works by first suppressing spin degrees of freedom with a large magnetic field then slowly changing the shape of the potential function separating the two dots using V_d . Once the potential barrier between the dots is large enough, the tunneling rate will become negligible.

Capacitive coupling between the probe dot and the pair of dots can be tuned such that occupation of the probe dot suppresses the degeneracy of the two-dot system. This is because the lowest energy state will occur when the two electrons are farthest apart. Thus, we can tune the system to a state where there is an entropy change of the entire thermodynamic system independent (while no change in entropy of the probe dot itself) as the probe dot changes occupation. In this way, we will be able to detect a non zero value of entropy if we are able to detect changes in entropy of a capacitively coupled system. Specifically, by tuning the upper two dot system between non-degenerate and doubly degenerate, we will be able to see the change as entropy as the probe dot transitions $0 \rightarrow 1$ electrons vary from $\Delta S = 0$ to

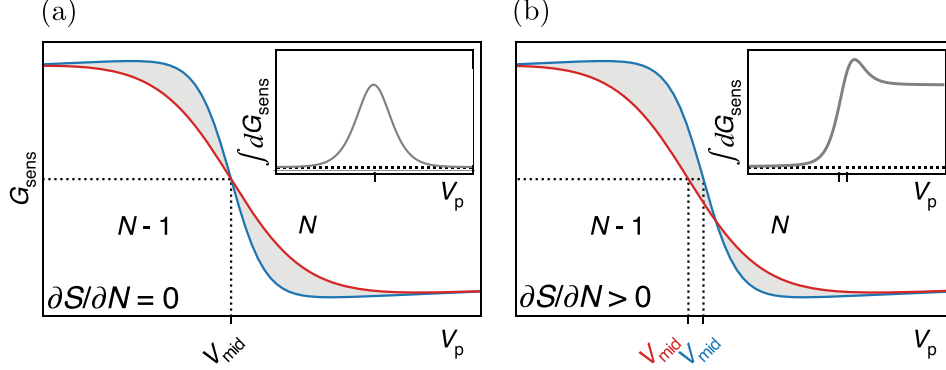


Figure 2.1: In (a) and (b) we show two examples of the measurement protocol where the occupancy of the probe dot is measured using G_{sens} . In each case, the occupancy is swept from $N - 1$ to N electrons both at a higher temperature (red) and a lower temperature (blue), however in (a) this change in N does not correspond to an entropy change in the system whereas in (b) we see a positive change in entropy of the system due to this change in occupancy. The inlaid plots show the cumulative integral of dG_{sens} – or the difference between hot and cold G_{sens} curves. The entropy change of the system is measured by the value of this integral after the completion of this transition. V_{mid} is labelled for each curve, notably, V_{mid} is the same in the zero entropy case, but shifts in the finite entropy case. Figure from Hartman et al.

$\Delta S = -\ln 2$, respectively.

2.3 Free energy explanation

To get a physical intuition for the thermodynamics at work to make this measurement possible, it may be useful to consider the Maxwell relation in Eqn.2.2 in terms of free energy of the system. More will be added here, specifically, a more complete explanation of the measurement in terms of free energy.

Chapter 3

Capacitively coupled double quantum dot

3.1 Quantum dots in GaAs/AlGaAs heterostructures

The focus of this section will be the theory of double (and single) quantum dots in the 2 dimensional electron gas hosted by AlGaAs/GaAs. The basis of this section will be the Fig. 3.1. In addition, there will be a discussion of the energy scales at play in the system and those that are most important for our entropy measurements.

3.2 The device and measurement protocol

The measurement protocol as laid out in Fig. 2.1 requires the ability to vary the temperature of the system. However, in practice, instability in the exact locations of V_{mid} makes it difficult to accurately determine ΔS of the hot and cold curves independently. Because of this instability, it is necessary to oscillate between hot and cold as we measure over the transition. With this measurement scheme, any heating not localized on the device is not useful as it will take too long to equilibrate through the entirety of whatever larger system is being heated.

We are pursuing multiple possible solutions for fast localized heating. The first is the technique employed by Hartman et al. and used in previous device designs which involves directly injecting hot electrons into the electron reservoir

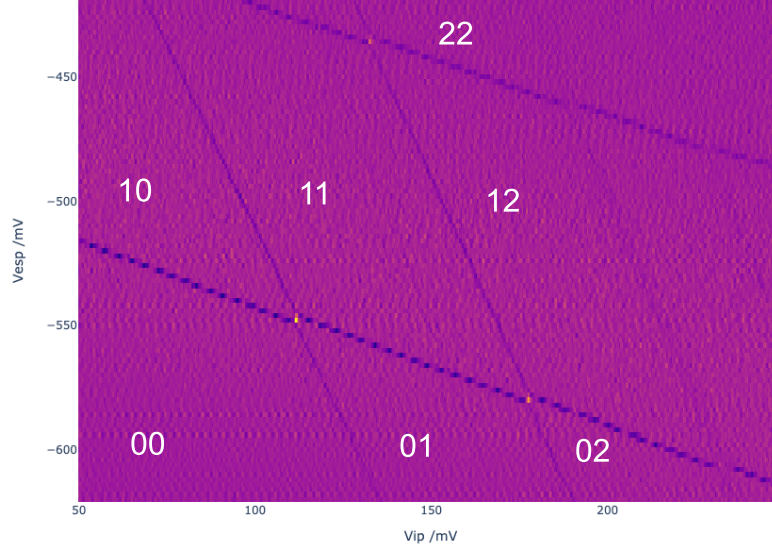


Figure 3.1: The states of the double quantum dot system are mapped out by charge sensing the occupation of both dots. The color indicates the derivative of the current through the charge sensor. Sudden changes in this current indicate state changes in the two dots, with larger changes (seen as darker on this plot) indicating changes in the probe dot, and smaller changes (slightly lighter on this plot) indicating changes in states in the impurity dot. The large squares indicate regions of constant state in the two dots and are labelled by [occupation main dot, occupation impurity dot].

coupled to the probe dot. This can be done by running a current through a QPC (tuned to be fairly resistive) pointed into the electron reservoir. When the current is turned off the heat in the electron reservoir is dissipated by coupling to phonons and connection to a ‘cold’ ground - i.e. a much larger bath of electrons at lower temperature. By turning on and off the current running through this resistive heater QPC, we can locally control the temperature of the electrons in the system. Another

possible technique that could be employed to allow for fast localized heating is heating the crystalline lattice of the substrate. With this technique, the electron-phonon coupling in the electron reservoir would ensure that the electrons quickly thermalize. Resistive heating would most likely be used to heat the phonons, either by electron phonon coupling using a QPC which is electrically insulated from the device, or by building a resistor on top of the substrate using a very long wire with some finite resistance.

Devices to complete this experiment will be built on GaAs/AlGaAs heterostructure which hosts a 2DEG (see Fig 3.6). The 2DEG is electrostatically gated to allow for local control of the electron density i.e. by applying an electric field with an electrically isolated gate, the electron density of the 2DEG is controlled beneath this gate [6]. Ohmic contact is made with the 2DEG via a diffusive process of Ni/Au/Ge through the substrate. Gating structures will be defined using standard photolithography and electron beam lithography techniques.

The next part of this section will focus on breaking down the various gates in use on the device and their roles. Relevant length scales, etc. will be discussed. This section is focussed around Fig. 3.2. Connections will be made to the previous section, pointing out the energy scales in our system and how they were calculated.

3.3 Results

The primary results are summarized in Fig. 3.3. These show the main focus of this thesis - that the entropy of a capacitively coupled quantum system can be probed directly within this scheme. More to be included in this section is a full explanation of these results. Ongoing work is going on probing the system in interesting regimes - i.e. looking for entropic signatures of the Kondo effect. It is possible that results relating to the Kondo effect will be found before this thesis is submitted.

More specifically, we have shown that we can measure a change in entropy in the second, capacitively coupled quantum dot, as the electron in the probe dot forces the electron in the second dot out. Rather than seeing a constant entropy at $\ln 2$, we see our ΔS go to zero in the center of the $01 \rightarrow 10$ transition, when the probe dot pushes the second quantum dot from a degeneracy of two (1 occupied electron, either spin up or spin down) to a degeneracy of 1 (0 electrons). This is

a net change in entropy of $-\ln 2$ in the second dot, and a net change in entropy of $+\ln 2$ in the probe dot, which cancel one another out.

3.4 Comparison to theory

The focus of this section will be a comparison between Fig. 3.3 and Fig. 3.5 and a qualitative explanation for the effects that we see. In addition, a discussion of the techniques used to make the theoretical predictions.

3.5 Conclusion

Not yet sure what the focus of this section will be, still thinking about it.

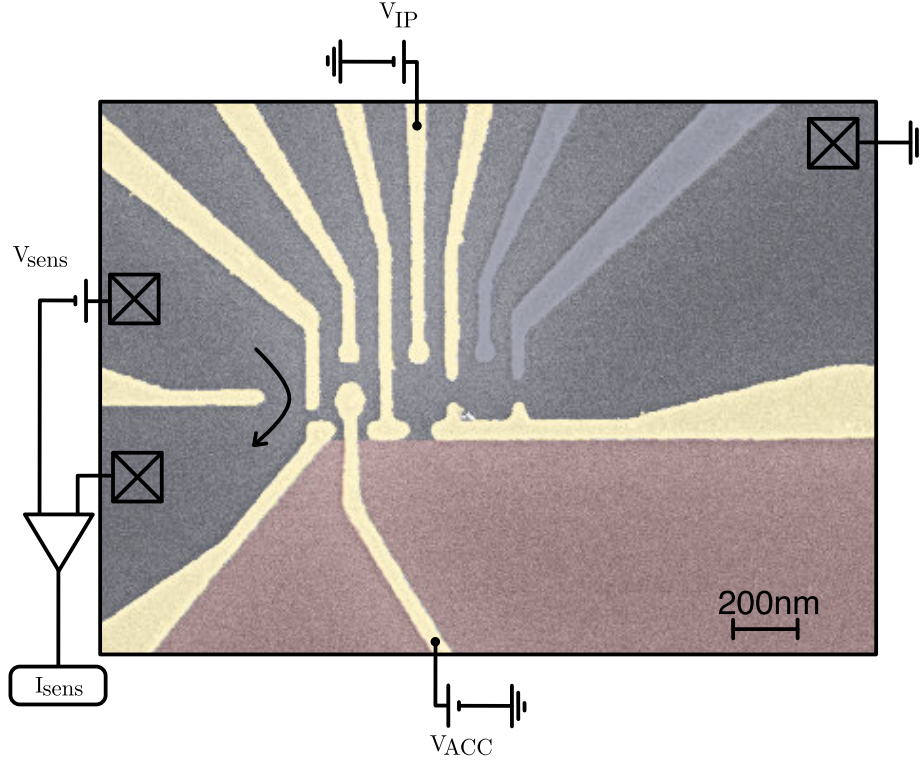


Figure 3.2: A top-down SEM image of the device measured in this experiment. Lighter gold regions are the gold gates, while darker regions are the GaAs substrate. A single quantum dot (right hand side) is probed by the leftmost dot whose occupation is measured using I_{sens} . In this device, temperature oscillations occur across electrons in a reservoir connected to the probe dot heated via a small thermocurrent through an adjacent quantum point contact. V_{ACC} is used to control the chemical potential, μ , in the probe dot. In the right hand of dot, similar gate structures, labelled V_{IP} allow for the system to be tuned to be tuned degenerate with the probe dot. The X indicates ohmic contact to the 2DEG. The light red section indicates the thermal reservoir of the system. Greyed out gates were not used in this experiment.

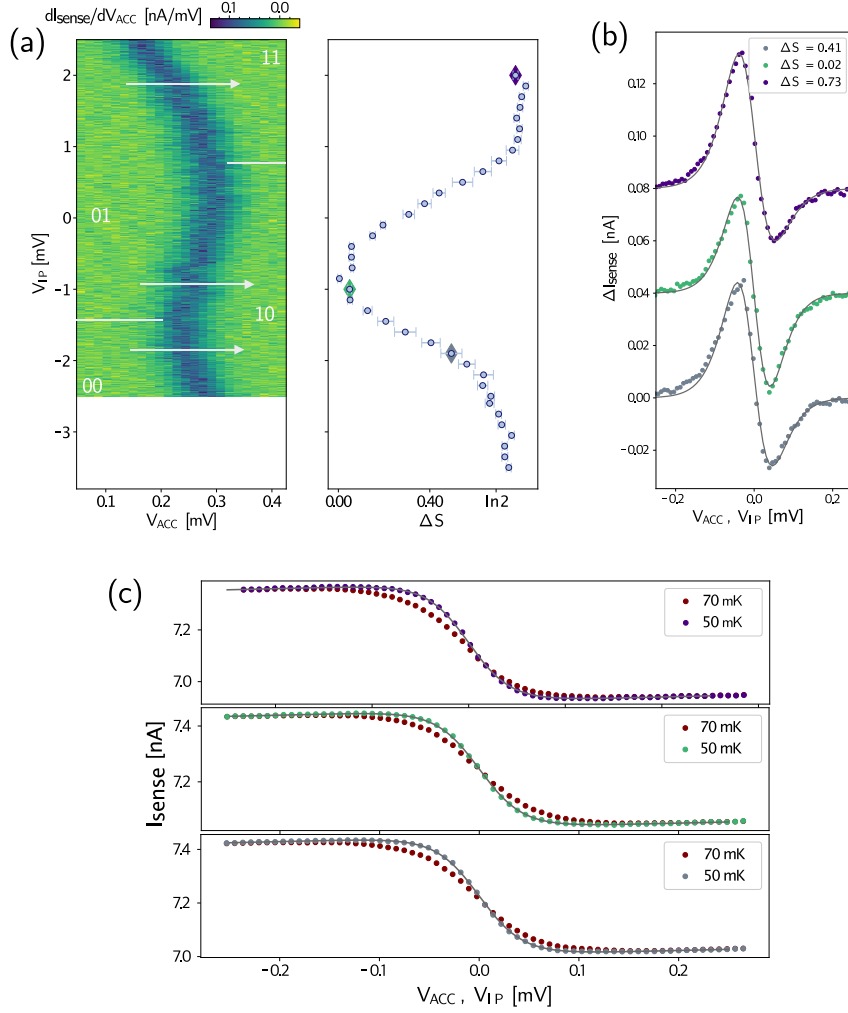


Figure 3.3: Entropy along the $0,1 \rightarrow 1,0$ transition in the pair of dots with $\Gamma_{\text{main}}/T < 1 < \Gamma_{\text{imp}}/T$. In (a) the dark region indicates the transition in the main quantum dot. Double dot states are labelled as [Occupation main dot, occupation impurity dot]. The ΔS of the transition in the main dot is plotted for the double dot transition crossing. In the $0,0 \rightarrow 1,0$ regime, the ΔS is found to be roughly $\ln 2 \approx 0.69$ as expected from the spin degeneracy in the probe dot. In the central regime, where there is a full $0,1 \rightarrow 1,0$ transition, entropy is found to be around $\ln 2 - \ln 2 = 0$ since the spin degeneracy of the impurity dot is simply replaced by the spin degeneracy in the probe dot. In (b) the ΔI between the cold and hot curves plotted in (c) are shown. In (c) the shift in V_{mid} between 70 mK and 50 mK traces can clearly be seen to vary depending on ΔS .

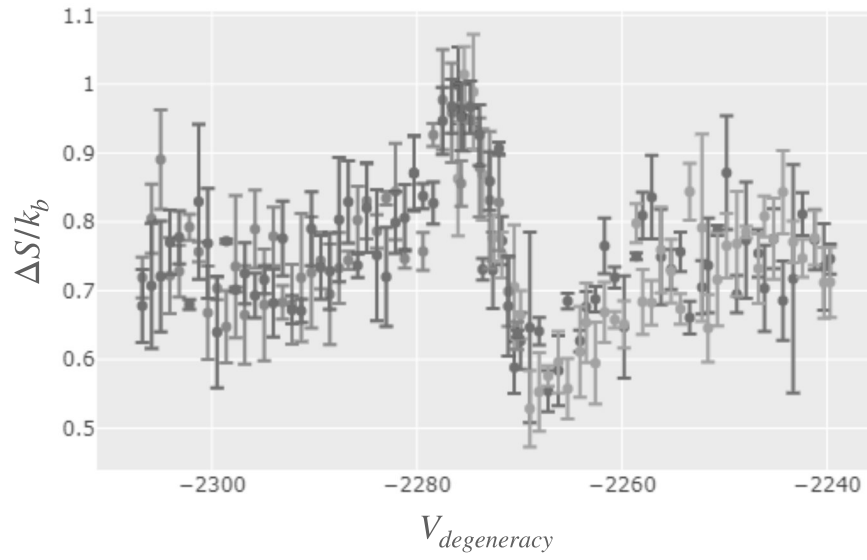


Figure 3.4: Data from an older device exhibits a change in entropy as degeneracy of an unknown external impurity is adjusted. The demonstrates the potential for measuring the entropy of capacitively coupled systems.

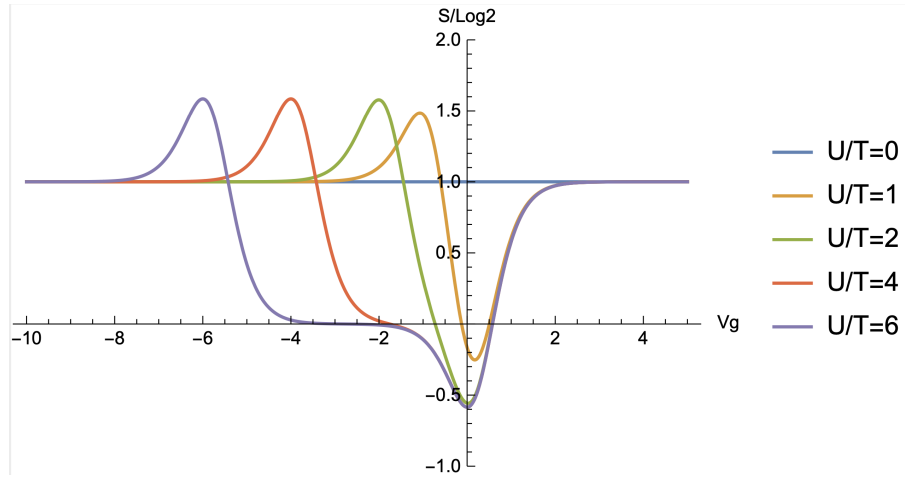


Figure 3.5: Theoretical calculations of ΔS across the $01 \rightarrow 10$ transition are shown for various levels of interdot capacitive coupling to temperature ratios. Excellent alignment with experiment is achieved in the $U/T = 6$ case.

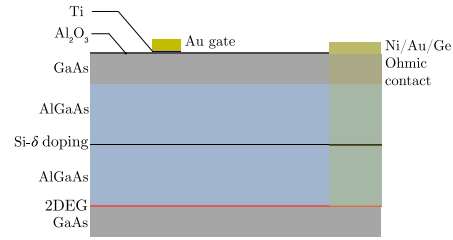


Figure 3.6: A cross section of the GaAs/AlGaAs heterostructure hosting a 2-dimensional electron gas (2DEG) formed at the boundary between an AlGaAs and GaAs layer where the conductance band briefly falls below the Fermi energy [3]. Gold gates allow local control of the electron density of the 2DEG. Ohmic contact to the 2DEG is established by a diffusion of a combination of Ni/Au/Ge from the surface to the 2DEG.

Bibliography

- [1] Fault-tolerant quantum computation by anyons. *Annals of Physics*, 303(1):2 – 30, 2003. ISSN 0003-4916.
doi:[https://doi.org/10.1016/S0003-4916\(02\)00018-0](https://doi.org/10.1016/S0003-4916(02)00018-0). → pages 1
- [2] N. W. Ashcroft and N. D. Mermin. *Solid State Physics*. Holt, Rinehart & Winston, New York ; London, 1976. → pages 4
- [3] S. Baer and K. Ensslin. *Transport Spectroscopy of Confined Fractional Quantum Hall Systems*. Springer International Publishing, 2015.
doi:10.1007/978-3-319-21051-3. → pages viii, 15
- [4] J. Elzerman, R. Hanson, L. W. Van Beveren, B. Witkamp, L. Vandersypen, and L. P. Kouwenhoven. Single-shot read-out of an individual electron spin in a quantum dot. *nature*, 430(6998):431–435, 2004. → pages 4
- [5] N. Hartman, C. Olsen, S. Lüscher, M. Samani, S. Fallahi, G. C. Gardner, M. Manfra, and J. Folk. Direct entropy measurement in a mesoscopic quantum system. *Nature Physics*, 14(11):1083–1086, 2018. → pages 1
- [6] L. P. Kouwenhoven, G. Schön, and L. L. Sohn. *Introduction to Mesoscopic Electron Transport*, pages 1–44. Springer Netherlands, Dordrecht, 1997.
doi:10.1007/978-94-015-8839-3_1. → pages 9
- [7] V. Mourik, K. Zuo, S. M. Frolov, S. R. Plissard, E. P. A. M. Bakkers, and L. P. Kouwenhoven. Signatures of majorana fermions in hybrid superconductor-semiconductor nanowire devices. *Science*, 336(6084): 1003–1007, 2012. ISSN 0036-8075. doi:10.1126/science.1222360. → pages 1
- [8] C. Nayak, S. H. Simon, A. Stern, M. Freedman, and S. Das Sarma. Non-abelian anyons and topological quantum computation. *Rev. Mod. Phys.*, 80:1083–1159, Sep 2008. doi:10.1103/RevModPhys.80.1083. → pages 1

- [9] I. Pomeranchuk. On the theory of liquid ^3He . *Zh. Eksp. Teor. Fiz.*, 20:919, 1950. → pages 2
- [10] R. M. Potok, I. G. Rau, H. Shtrikman, Y. Oreg, and D. Goldhaber-Gordon. Observation of the two-channel kondo effect. *Nature*, 446(7132):167–171, 2007. doi:10.1038/nature05556. → pages 1
- [11] A. Rozen, J. M. Park, U. Zondiner, Y. Cao, D. Rodan-Legrain, T. Taniguchi, K. Watanabe, Y. Oreg, A. Stern, E. Berg, P. Jarillo-Herrero, and S. Ilani. Entropic evidence for a pomeranchuk effect in magic-angle graphene. *Nature*, 592(7853):214–219, 2021. doi:10.1038/s41586-021-03319-3. URL <https://doi.org/10.1038/s41586-021-03319-3>. → pages 2
- [12] Y. Saito, F. Yang, J. Ge, X. Liu, T. Taniguchi, K. Watanabe, J. I. A. Li, E. Berg, and A. F. Young. Isospin pomeranchuk effect in twisted bilayer graphene. *Nature*, 592(7853):220–224, 2021. doi:10.1038/s41586-021-03409-2. URL <https://doi.org/10.1038/s41586-021-03409-2>. → pages 2
- [13] D. Schroeder. *An Introduction to Thermal Physics*. Addison Welsley Longman, 2000. → pages 3, 4
- [14] E. Sela, Y. Oreg, S. Plugge, N. Hartman, S. Lüscher, and J. Folk. Detecting the universal fractional entropy of majorana zero modes. *Phys. Rev. Lett.*, 123:147702, Oct 2019. doi:10.1103/PhysRevLett.123.147702. → pages 1
- [15] Z. Su, A. Zarassi, J.-F. Hsu, P. San-Jose, E. Prada, R. Aguado, E. J. H. Lee, S. Gazibegovic, R. L. M. Op het Veld, D. Car, S. R. Plissard, M. Hocevar, M. Pendharkar, J. S. Lee, J. A. Logan, C. J. Palmstrøm, E. P. A. M. Bakkers, and S. M. Frolov. Mirage andreev spectra generated by mesoscopic leads in nanowire quantum dots. *Phys. Rev. Lett.*, 121:127705, Sep 2018. doi:10.1103/PhysRevLett.121.127705. → pages 1
- [16] R. Willett, J. P. Eisenstein, H. L. Störmer, D. C. Tsui, A. C. Gossard, and J. H. English. Observation of an even-denominator quantum number in the fractional quantum hall effect. *Phys. Rev. Lett.*, 59:1776–1779, Oct 1987. doi:10.1103/PhysRevLett.59.1776. → pages 1

Appendix A

Measurement technique

A.1 Heating

This section will be devoted to the following topics:

1. The circuit design to achieve mK level broadening in the thermal reservoir while preventing any potential from developing in the reservoir, which would effectively shift the chemical potential of the reservoir.
2. Techniques used to apply synchronously apply two, 90° out of phase square wave heating signals on either side of a remote quantum point contact, allowing for heating in separate bath while preventing a monopole electric moment from affecting the entropy measurement.

A.2 Extraction of dN/dT signal

This section will be devoted to the following topics:

1. The techniques used to allow for repeated measurements and used to fit and extract entropy signals.

A.3 Artifacts from cross couplings

The focus of this section will be explanations of the artifacts that are notably present in dN/dT data presented in this thesis. See

A.4 Determination of electron temperature

This section will focus on methods for determination of electron temperature in this system as well as the methodology we have employed to achieve these temperatures. With specific reference to Fig. A.1.

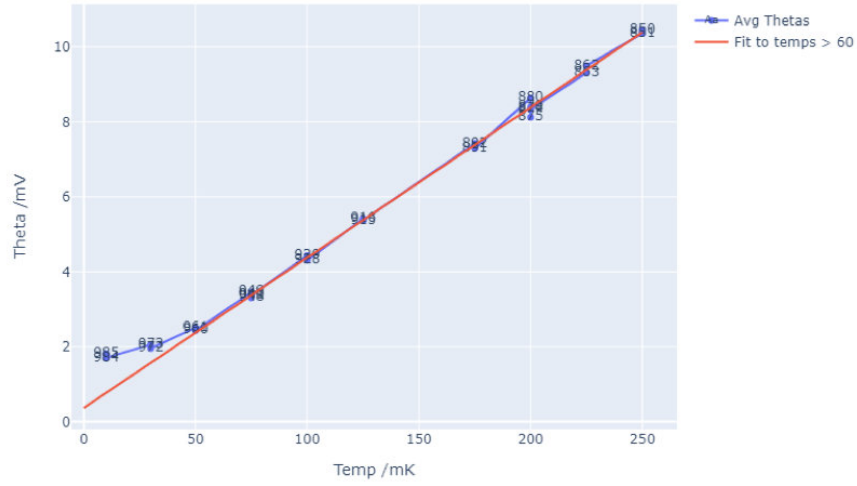


Figure A.1: By fitting the transition line shapes of the $0 \rightarrow 1$ electron transition in the quantum dot, one can extract the broadening of the fermi energy in the reservoir. By varying the lattice temperature of the substrate and plotting the effective broadening of the fermi sea (θ) at each lattice temperature, we can extract the effective electron temperature, T_e . Here $T_e \approx 35$ mK.

Appendix B

Measurement setup

This section will include

- Detailed description of experimental techniques by which data are collected
- Samples of multiple levels of data through processing

Appendix C

Device Fabrication

This section will include

- Processes which are followed for the production of devices on a GaAs substrate
- Various check lists for processes (space depending).

To fabricate the devices referred to in this thesis and previous iterations of similar devices, a number of nano-fabrication recipes were developed and iterated upon. In this section, these processes are described and recipes used are laid out.